

CHARACTERIZATION OF CHRYSOTILE, ANTIGORITE AND LIZARDITE BY FT-RAMAN SPECTROSCOPY

CATERINA RINAUDO[§] AND DANIELA GASTALDI

*Dipartimento di Scienze e Tecnologie Avanzate, Università del Piemonte Orientale "Amedeo Avogadro",
Corso Borsalino 54, I-15100 Alessandria, Italy*

ELENA BELLUSO

Dipartimento di Scienze Mineralogiche e Petrologiche, Università di Torino, Via Valperga Caluso 35, I-10125 Torino, Italy

ABSTRACT

We analyzed samples of antigorite, lizardite and fibrous chrysotile, three representative minerals of the serpentine group, to determine their chemical and structural properties, and their FT-Raman spectra. The low-frequency region of the spectrum (1200–200 cm^{-1}), which corresponds to the lattice-vibration modes, was then analyzed, and the observed bands attributed, on the basis of our results. Raman spectroscopy thus proves useful in identifying the three mineral species, despite their strong similarities in structure and chemical composition. The symmetric stretching modes of the Si–O_b–Si linkages vibrate at different frequencies in chrysotile and antigorite, whereas chrysotile and lizardite can easily be identified by analyzing the vibrations of the OH–Mg–OH groups and the bands in the range 550–500 cm^{-1} .

Keywords: Raman spectroscopy, asbestos, serpentine-group minerals, chrysotile, antigorite, lizardite.

SOMMAIRE

Nous avons analysé des échantillons d'antigorite, de lizardite et de chrysotile fibreuse, trois minéraux représentatifs du groupe de la serpentine, afin d'en déterminer les propriétés chimiques et structurales, et leurs spectres de Raman avec transformation de Fourier. La région du spectre à faible fréquence (1200–200 cm^{-1}), qui correspond aux modes de vibration du réseau, a été analysée, et les bandes observées ont été attribuées. Les spectres s'avèrent ainsi utiles dans l'identification des trois espèces, malgré leurs grandes ressemblances structurales et compositionnelles. Les modes d'étirement symétriques des agencements Si–O_b–Si vibrent à des fréquences différentes dans le chrysotile et l'antigorite, tandis que chrysotile et lizardite sont facilement identifiables par analyse des vibrations des groupes OH–Mg–OH et des bandes dans l'intervalle 550–500 cm^{-1} .

(Traduit par la Rédaction)

Mots-clés: spectroscopie de Raman, minéraux asbestiformes, minéraux du groupe de la serpentine, chrysotile, antigorite, lizardite.

INTRODUCTION

The three principal minerals of the serpentine group, chrysotile, antigorite and lizardite, have a very similar chemical composition, but significantly different structures. In fact, the single ideal chemical formula $(\text{OH})_3\text{Mg}_3[\text{Si}_2\text{O}_5(\text{OH})]$ corresponds to several crystal structures that represent different solutions for the minimization of the mismatch between sheets of SiO_4 tetrahedra and sheets of $\text{MgO}_2(\text{OH})_4$ octahedra. In lizardite, the resulting structure is planar, owing to shifts of the

octahedral and tetrahedral cations away from their ideal positions and to the limited Al-for-Si substitution in the tetrahedral sites. In antigorite, the misfit is compensated by an alternating-wave structure in which the sheet of octahedra is continuous, whereas the SiO_4 tetrahedra are tilted and periodically switch their orientation, pointing alternatively in opposite directions. Finally, chrysotile has a coiled structure, which is responsible for its properties as asbestos (Wicks & Whittaker 1975, Wicks & O'Hanley 1988, Veblen & Wylie 1993).

[§] E-mail address: caterina.rinaudo@unipmn.it

Naturally occurring intergrowths of three types of serpentine minerals are very common. It is thus of great interest to find an experimental technique that permits identification of the mineral species without long and costly preparation of the sample. Raman spectroscopy fits these criteria: it is a simple and rapid technique, and necessitates no sample preparation. It has been used successfully by a number of investigators in the study of chrysotile (Lewis *et al.* 1996, Bard *et al.* 1997, Klopogge *et al.* 1999), but only one bibliographic reference has been found concerning its use in the identification of antigorite and lizardite (Pasteris & Wopenka 1987). In this latter work, no attribution for the bands is made to the vibrational modes of the groups constituting the crystal structure.

In order to identify the Raman vibrations that are specific to each serpentine phase studied and that would permit rapid recognition of the mineral, several specimens of the three species were examined. Before characterization by Raman spectroscopy, the crystallographic and chemical properties of each sample were established using the techniques of X-ray powder diffraction (XRD), scanning electron microscopy (SEM), transmission electron microscopy (TEM), analytical electron microscopy (AEM), and energy-dispersion spectrometry (EDS).

EXPERIMENTAL

Some of the samples of chrysotile studied were provided by NIST (National Institute of Standards and Technology). Others were taken from the reference collections of the Dipartimento di Scienze Mineralogiche e Petrologiche, Università di Torino, and are found in outcrops of rocks rich in serpentine minerals in the Piedmont Alps, Italy.

All of the samples of antigorite studied were taken from the Dipartimento di Scienze Mineralogiche e Petrologiche, Torino, and come from the same areas mentioned above.

The sample of lizardite in the study comes from Monte Fico, Elba Island, Italy; its structural and chemical properties were studied previously by Mellini & Viti (1994), and the sample was kindly provided by Professor Mellini.

For the XRD analyses, the samples were powdered in an agate mortar. No problems were encountered with the antigorite or lizardite, but chrysotile fibers needed to be cut with scissors before crushing, as they are so flexible and soft.

Each powdered sample was mounted on a flat holder and examined initially by the powder method using a Siemens D5000 X-ray diffractometer equipped with $\text{CuK}\alpha$ radiation. The EVA software program was used to determine the mineral phases present in each X-ray powder spectrum, by comparing the experimental peaks with PDF2 reference patterns.

As the XRD spectra are very similar for minerals with such similar chemical and crystallographic properties, more precise characterization of each sample was performed by transmission electron microscopy (Philips CM12 instrument, operated at 120 kV); they were chemically analyzed with the attached EDS microprobe [EDAX Si(Li) detector PV9800]. The standardless SUPQ program was used with the default K factors to process the chemical data; the final values were obtained as normalized proportion of oxides (wt.%). The samples were prepared by suspending the powder in isopropyl alcohol, and the suspension then underwent ultrasound treatment in order to minimize fiber aggregation; finally, several drops of the suspension were deposited on a carbon-supported Cu grid.

The percentage of each mineralogical phase detected in the XRD spectrum was easily calculated using the EVA support program, which compares the area and intensity of two diffraction peaks, each diagnostic of one mineral component of the mixture. It is worth noting that the calculated values are reliable in powdered specimens without preferred orientation of the component crystallites. In our case, especially for chrysotile, some preferred orientation of the fibers certainly was present. The percentages calculated on the basis of the XRD spectra were therefore compared with the data obtained using TEM and AEM. In this case, selected-area electron diffraction (SAED) patterns and EDS-TEM chemical analyses of each point examined permitted conclusive attribution to the mineral phase. Many crystals and different points within a single bundle of fibers from each specimen of chrysotile and antigorite were analyzed by SAED and EDS-TEM. Thus it was possible to calculate the proportion of each coexisting mineral phase.

A morphological study was performed with a Cambridge Stereoscan 360 SEM: the samples were glued onto aluminum stubs with colloidal graphite and then coated with a carbon film approximately 400 Å in thickness.

Finally, the serpentine phases were studied in a back-scattering geometry with a Bruker RFS100 FT-Raman spectrometer equipped with an Nd:YAG laser at an excitation wavelength of 1064 nm, and a Ge detector, which requires liquid N_2 for cooling. The advantage in using a laser operating at near-infrared radiation is that the fluorescence from the sample is reduced, heating and phase transition are avoided, and measurements are made possible for longer periods of time. All the spectra of each mineral were recorded on several mg of powdered sample. Random orientation of the crystallites in the powder analyzed was achieved only with the antigorite and lizardite samples; in the case of chrysotile, some preferred orientation of the fibrils is impossible to avoid. The Raman spectra were obtained at a 2 cm^{-1} resolution and by adapting the laser power and number of scans in order to optimize the signal-to-noise

ratio: 2000 scans over 100 minutes and 120 mW were sufficient in order to obtain the optimum resolution.

Internal calibration of the Raman spectrometer was assured by a reference He-Ne laser (632.8 nm). The accuracy of the band position was also checked by measuring the center wavenumber of two Stokes and anti-Stokes bands at low frequencies: if everything is correctly calibrated, they are equal.

In this work, only the Raman region related to lattice-vibrational modes ranging from 1200 to 200 cm^{-1} was analyzed.

RESULTS AND DISCUSSION

The three species of serpentine considered in this work are commonly found in a single specimen; several samples were tested, especially for chrysotile and antigorite. The samples selected for Raman spectroscopy satisfied the criterion of having one largely predominant phase, as revealed by XRD, TEM and AEM studies. The chrysotile, antigorite and lizardite specimens selected showed the presence of other phases as well, but in minor amounts.

The chrysotile sample chosen accounts for about 95%, and antigorite, for about 5% of the whole sample. The chemical composition of the chrysotile fibers in the sample studied was established by several analyses performed under TEM by AEM on the selected areas, and

proved to be: $(\text{Mg}_{11.70}\text{Al}_{0.08}\text{Fe}_{0.22})_{\Sigma 12.00}(\text{Si}_{7.98}\text{Al}_{0.02})_{\Sigma 8.00}\text{O}_{20}(\text{OH})_{16}$.

XRD and TEM analyses of the antigorite sample chosen for Raman characterization revealed an almost pure antigorite; no more than 3% of chrysotile was found to be present. AEM analyses indicated a chemical composition of: $(\text{Mg}_{11.05}\text{Fe}_{0.53}\text{Al}_{0.21})_{\Sigma 11.79}\text{Si}_{8.05}\text{O}_{20}(\text{OH})_{16}$.

For the lizardite analyzed by Raman spectroscopy, Mellini & Viti (1994) reported the composition: $(\text{Mg}_{10.96}\text{Fe}_{0.64}\text{Al}_{0.36})_{\Sigma 11.96}(\text{Si}_{7.72}\text{Al}_{0.28})_{\Sigma 8}\text{O}_{20}(\text{OH})_{16}$. XRD patterns indicated that the lizardite is mixed with a very small amount of chrysotile (about 5%).

The samples chosen, as studied by optical microscopy and by SEM, revealed the morphology represented in Figures 1a–c. The chrysotile, as shown in Figure 1a, is made up of thin and flexible fibrils, classifiable as asbestos because of their length:diameter ratio, which is >3 (Davis 1993); antigorite exhibits the columnar habit shown in Figure 1b, and lizardite has the plate-like morphology shown in Figure 1c.

The samples were studied last by Raman spectroscopy; for each sample, several spectra were registered on small quantities of ground material. Figure 2 shows a Raman spectrum obtained on the chrysotile sample of Figure 1a. The spectrum is characterized by the following main bands, assigned according to the description of the vibrational bands in the IR spectra of the

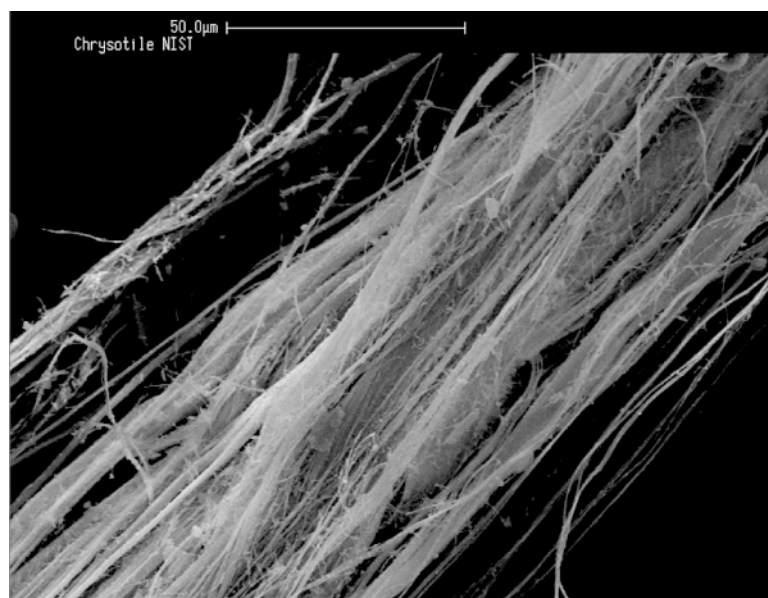


FIG. 1a. Secondary electron SEM image of the chrysotile studied by Raman spectroscopy. The flexibility of the constituent fibers is evident. Scale bar: 50 μm .

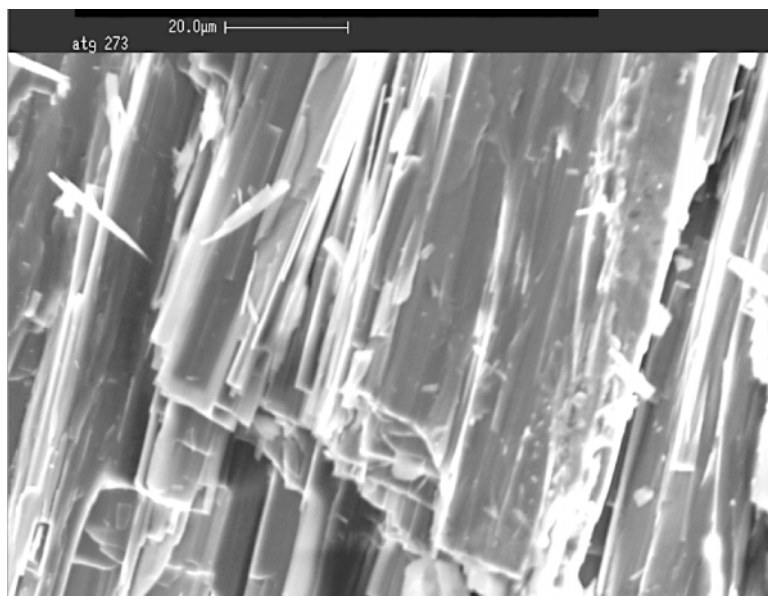


FIG. 1b. Secondary electron SEM image of the antigorite sample studied by Raman spectroscopy. The sample shows a columnar habit. Scale bar: 20 μm.

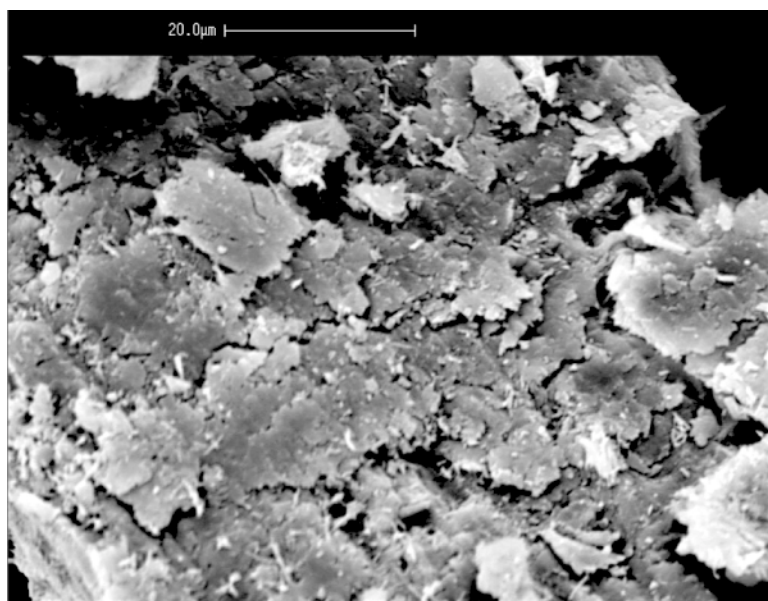


FIG. 1c. Secondary electron SEM image of the lizardite sample studied by Raman spectroscopy. Scale bar: 20 μm.

phyllosilicates proposed by Lazarev (1972) and Farmer (1974), and to the assignment for Raman bands in tubular chrysotile, as suggested by Klopogge *et al.* (1999):

1) a band at 1105 cm^{-1} , attributed to antisymmetric stretching modes (ν_{as}) of the Si–O_{nb} groups;

2) an intense band at 692 cm^{-1} , attributed to the symmetric stretching mode (ν_{s}) of the Si–O_b–Si groups;

3) a band at 620 cm^{-1} produced, following Klopogge *et al.* (1999), by OH–Mg–OH translation modes on the basis of the assignment of the band at 627 cm^{-1} observed on the infrared spectrum of brucite. On the other hand, Farmer (1974, p. 348) also attributed the strong bands observed in the chrysotile and antigorite IR spectra near $618\text{--}646\text{ cm}^{-1}$ to vibrations of the inner and surface hydroxyl groups of the layers;

4) two bands at 389 and 345 cm^{-1} , in a region of the spectrum where bending vibrations of the SiO₄ tetrahedra appear. The first one was assigned by Klopogge *et al.* (1999) to the $\nu_5(\text{e})$ bending modes of the SiO₄ tetrahedra. However, two bands at 379 and 353 cm^{-1} have also been detected previously in nontronite from Hohen-Hagen, Germany, and ascribed to bending vibrations of the SiO₄ units (Frost & Klopogge 2000);

5) one band lying at 231 cm^{-1} in a region of the spectrum where vibrations of the O–H–O groups are expected [O is the non-bridging oxygen atom of the tetrahedron SiO₄, and H is the hydrogen atom of the OH group tilted toward an octahedral cation vacancy (Griffith 1969, Loh 1973). In the dioctahedral phyllosilicates, where normally one third of the octahedral sites are vacant, the O–H–O groups form isosceles triangles. The Raman-active vibrational modes in an isosceles triangle are: symmetric stretching (ν_1) at 262 cm^{-1} , symmetric bending (ν_2) at 187 cm^{-1} , and antisymmetric stretching (ν_3) at 240 cm^{-1} (Loh 1973). In fact, in the FT-Raman spectrum of the dioctahedral phyllosilicates studied, kaolinite, dickite, halloysite and nontronite, two bands near $270\text{--}290$ and 240 cm^{-1} are observed and

assigned, respectively, to A₁(ν_1) and B₂(ν_3) vibrations of the O–H–O groups (Frost 1995, 1997, Frost & Kristof 1997). In trioctahedral phyllosilicates, the occupancy of almost all the octahedral sites by divalent cations prevents the formation of an O–H–O isosceles triangle. This fact changes the symmetry of the O–H–O groups; only one band is observed in the $200\text{--}300\text{ cm}^{-1}$ range in the spectra of the trioctahedral phyllosilicates studied. Nevertheless, assignment of this band to a precise vibrational mode of the O–H–O groups requires polarization of Raman measurements, and is, therefore, impossible for the moment.

In Figure 3, we report a Raman spectrum obtained on the antigorite sample shown in Figure 1b; on the whole, the spectrum appears more disturbed by noise; the main bands already observed in the previous spectrum may be found again, but lying at different frequencies. We see:

1) a band occurring at 1044 cm^{-1} that may correspond to the band observed in the IR reflection spectrum of this mineral at 1048 cm^{-1} and ascribed by Lazarev (1972, p. 123) to antisymmetric stretching modes (ν_{as}) of the Si–O_b–Si groups (E₁) and to the band detected in Raman spectrum of talc at 1049 cm^{-1} by Rosasco & Blaha (1980) and also ascribed to antisymmetric stretching vibrations of Si–O_b–Si groups;

2) an intense band at 683 cm^{-1} produced by symmetric stretching modes (ν_{s}) of the Si–O_b–Si linkages;

3) a band at 635 cm^{-1} ascribed, as for chrysotile, to the OH–Mg–OH translation modes. The shift of these vibrations in the two spectra may be correlated with the higher content of Fe or Al rather than Mg in the sheets of octahedra, as demonstrated by AEM analyses;

4) the band due to $\nu_5(\text{e})$ modes of the SiO₄ tetrahedra lies here at 375 cm^{-1} , a slightly lower frequency than in the chrysotile. Note that in chrysotile spectrum obtained by Klopogge *et al.* (1999), a strong band at 388 cm^{-1} lies near another band at 374 cm^{-1} . In this case,

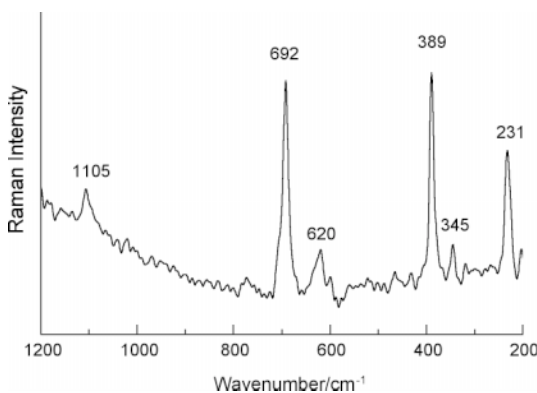


FIG. 2. An FT-Raman spectrum obtained for the chrysotile sample in Figure 1a.

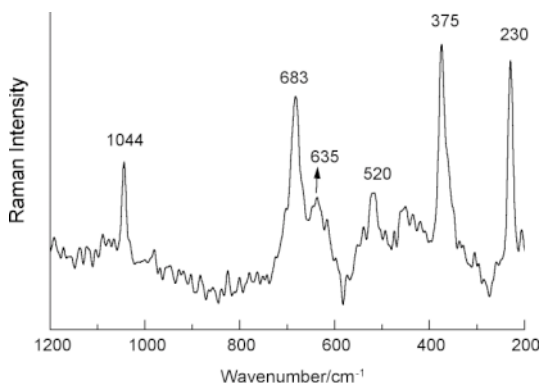


FIG. 3. An FT-Raman spectrum obtained for the antigorite sample in Figure 1b.

Kloprogge *et al.* (1999) suggested for the intense band at 388 cm^{-1} a $\nu_5(\text{e})$ mode of the SiO_4 tetrahedra, and for the band at 374 cm^{-1} , vibrations of the Mg–OH groups. In the spectrum of chrysotile that we obtained, no band at 374 cm^{-1} is observed (Table 1, Fig. 3a); only the vibrational modes of SiO_4 tetrahedra at 389 cm^{-1} are detected as a strong band. In the spectrum of antigorite, the intensity of the band at 375 cm^{-1} is comparable to that of the band at 389 cm^{-1} in the chrysotile spectrum; in our opinion, this band can therefore be ascribed to bending modes of SiO_4 tetrahedra.

5) there is no significant difference in the band near 230 cm^{-1} compared to the chrysotile spectrum; as discussed above, it derives from the vibrations of the O–H–O groups.

The band occurring in the chrysotile spectrum at 346 cm^{-1} is not present in antigorite; moreover, an additional band at 520 cm^{-1} is detected. Samples of talc show a Raman band of weak intensity at 519 cm^{-1} (Blaha & Rosasco 1978, Rosasco & Blaha 1980) and in the IR spectrum a band at 530 cm^{-1} . The latter is assigned by Lazarev (1972, p. 122) to deformation vibrations of the silicon–oxygen layer. Similarly, we propose that the band observed in the antigorite spectrum at 519 cm^{-1} be assigned to the deformation modes of the SiO_4 tetrahedra. In fact, as is typical in the antigorite structure, the sheet of tetrahedra periodically switches its orientation, and deformations of the SiO_4 tetrahedra at the reversal zone have been proposed.

In Figure 4, the Raman spectrum from the lizardite shown in Figure 1c is represented. The bands produced by vibrations of the SiO_4 tetrahedra or by silicon–oxygen linkages appear here at frequencies very close to those detected in the chrysotile spectra. In fact, the modes due to symmetric stretching (ν_s) of the Si–O_b–Si linkages lie here at 690 cm^{-1} (692 cm^{-1} in chrysotile), and the $\nu_5(\text{e})$ modes of the SiO_4 tetrahedra appear here at 388 cm^{-1} (389 cm^{-1} in chrysotile). The relative inten-

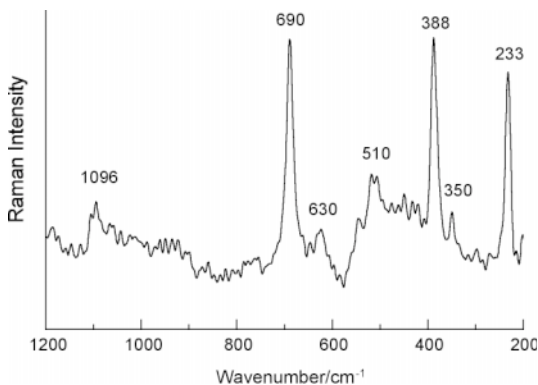


FIG. 4. An FT-Raman spectrum obtained for the lizardite sample in Figure 1c.

sities of these bands in the spectra shown in Figures 2 and 4 are also comparable. On the contrary, the anti-symmetric stretching modes (ν_{as}) of the Si–O_{nb}, which appear as a clear band at 1105 cm^{-1} in the chrysotile spectrum, here produce a weak and dubious band at 1096 cm^{-1} . When we now take into consideration the vibrations of OH–Mg–OH groups, they appear to be shifted to higher frequencies on the lizardite spectrum, 630 cm^{-1} , when compared to the vibrations of the same groups in chrysotile, 620 cm^{-1} . This shift, as discussed for antigorite, may be related to the higher content of Al and Fe, rather than Mg, in the layer of octahedra.

A band near 510 cm^{-1} has also been detected in the Raman spectrum of lizardite. It occurs in a frequency range where no band appears in the chrysotile spectrum. This band is observed in all spectra of lizardite recorded, and it seems to be made up of two bands lying at 506 and 515 cm^{-1} . In agreement with the assignment of the band at 520 cm^{-1} in the antigorite spectrum, an assign-

TABLE 1. ASSIGNMENT OF BANDS IN THE RAMAN SPECTRA OF THE THREE SERPENTINE PHASES STUDIED IN THIS WORK COMPARED WITH RESULTS OBTAINED ON CHRYSOTILE BY KLOPROGGE *et al.* (1999)

Band assignment	Chrysotile*	Chrysotile	Antigorite	Lizardite
$\nu_{\text{as}}\text{ Si-O}_{\text{nb}}$	1102	1105 m	–	1096 ?
$\nu_{\text{as}}\text{ Si-O}_{\text{b}}\text{-Si}$	–	–	1044 s	–
Mg–OH outer symmetric translation modes	709 705	– –	– –	– –
$\nu_s\text{ Si-O}_{\text{b}}\text{-Si}$	692	692 vs	683 vs	690 vs
Antisymmetric OH–Mg–OH translation modes	– 629 622	– – 620 m	635 m – –	630 m – –
Libration of inner Mg–OH	607	–	–	–
$\text{SiO}_4\text{-AlO}_4$ deformation modes	–	–	520 m	510 m (506, 515)
Mg–OH translation + $\nu_5(\text{e})\text{ SiO}_4$	466	–	–	–
$\nu_2(\text{a})_2\text{SiO}_4$	458	–	–	–
Antisymmetric Mg–OH translation	432	–	–	–
Symmetric $\nu_5(\text{e})\text{ SiO}_4$	388	389 vs	375 vs	388 vs
Symmetric Mg–OH vibrations	374	–	–	–
Bending of SiO_4	345 318 304	345 m – –	– – –	350 m – –
Vibrations of O–H–O groups	231	231 s	230 vs	233 vs
$A_1\text{g mode of Mg (O,OH)}_6$	199	–	–	–

vs: very strong; s: strong; m: medium; w: weak; sh: shoulder. The frequency of the bands is quoted in cm^{-1} . * Kloprogge *et al.* (1999).

ment to deformation vibrations of the $\text{SiO}_4\text{-AlO}_4$ tetrahedra may be proposed. In fact, in the structure of lizardite, the mismatch between the layers of tetrahedra and octahedra is compensated by deviation of the sheet of tetrahedra from an ideal hexagonal symmetry to a ditrigonal arrangement with tilting of the tetrahedra of about -2.8° and by a more substantial substitution of Al-for-Si in the layer of tetrahedra (Mellini 1982, Mellini & Viti 1994). The splitting of the band at about 510 cm^{-1} into two bands at 509 and 516 cm^{-1} may therefore reflect deformation vibrations of the two types of tetrahedra, AlO_4 and SiO_4 .

In Table 1, the bands observed in the spectra of the three minerals studied are reported and compared with the results obtained on chrysotile by Klopogge *et al.* (1999).

CONCLUSIONS

On the basis of our findings, Raman spectroscopy provides a reliable and simple-to-perform technique for distinguishing among the three common phases of serpentine, chrysotile, antigorite and lizardite. In fact, after comparing the spectra shown in Figures 2, 3 and 4, we conclude that:

a) the frequencies of the stretching modes of $\text{Si-O}_b\text{-Si}$ and Si-O_{nb} linkages allow chrysotile to be distinguished unequivocally from antigorite (ν_s and ν_{as} of antigorite less than ν_s and ν_{as} of chrysotile);

b) chrysotile and lizardite are easily distinguishable in the region where the frequencies of the bands produced by the vibrations of the OH-Me-OH groups occur. In fact, the spectrum of lizardite closely resembles that of chrysotile where the different silicon-oxygen or SiO_4 tetrahedra vibrations occur, but it resembles the antigorite spectrum where the vibrations of the octahedrally coordinated cations linked to OH occur. Moreover, another clue to identifying the mineral phase can be found in the presence in the lizardite spectrum of a band (actually a double band) near 510 cm^{-1} in the range of $550\text{-}500\text{ cm}^{-1}$, in a region where no band has been observed in the chrysotile spectrum by us or other research groups (Lewis *et al.* 1996, Bard *et al.* 1997, Klopogge *et al.* 1999).

c) antigorite and lizardite are easily distinguishable from one another on the basis of their ν_s and ν_{as} frequencies of the silicon-oxygen bonds. Both these minerals show bands in the range of $550\text{-}500\text{ cm}^{-1}$. The fact that these bands are detected only in the spectra of lizardite and antigorite, where the normal development of the sheet of tetrahedra is structurally disturbed (in the first case by switching, in the second by tilting and by Al-for-Si substitution), also suggests that these bands should be assigned to deformed modes of the SiO_4 and AlO_4 tetrahedra.

ACKNOWLEDGEMENTS

The authors are grateful to Professor M. Mellini of the Università di Siena, who kindly provided the lizardite sample, Professor P.L. Stanghellini of the Università di Piemonte Orientale and Professor Sidney F.A. Kettle for the helpful discussions. A particular thanks also goes to the referees and to Associate Editor Mickey Gunter for their work.

REFERENCES

- BARD, T., YARWOOD, J. & TYLEE, B. (1997): Asbestos fiber identification by Raman microspectroscopy. *J Raman Spectrosc.* **28**, 803-809.
- BLAHA, J.J. & ROSASCO, G.J. (1978): Raman microprobe spectra of individual microcrystals and fibers of talc, tremolite, and related silicate minerals. *Anal. Chem.* **50**, 892-896.
- DAVIS, J.M.G. (1993): *In vivo* assays to evaluate the pathogenic effects of minerals in rodents. In *Health Effects of Mineral Dusts* (G.D. Guthrie Jr. & B.T. Mossman, eds.). *Rev. Mineral.* **28**, 471-487.
- FARMER, V.C. (1974): *The Infrared Spectra of Minerals*. The Mineralogical Society, London, U.K.
- FROST, R.L. (1995): Fourier transform Raman spectroscopy of kaolinite, dickite and halloysite. *Clays Clay Minerals* **43**, 191-195.
- _____ (1997): The structure of the kaolinite minerals – a FT-Raman study. *Clay Minerals* **32**, 65-77.
- _____ & KLOPOTOGGE, J.T. (2000): Raman spectroscopy of nontronites. *Appl. Spectrosc.* **54**, 402-405.
- _____ & KRISTOF, J. (1997): Intercalation of halloysite: a Raman spectroscopic study. *Clays Clay Minerals* **45**, 551-563.
- GRIFFITH, W.P. (1969): Raman studies on rock-forming minerals. I. Orthosilicates and cyclosilicates. *J. Chem. Soc. (A)* **9**, 1372-1377.
- KLOPOTOGGE, J.T., FROST, R.L. & RINTOUL, L. (1999): Single crystal Raman microscopic study of the asbestos mineral chrysotile. *Physical Chemistry, Chemical Physics* **1**, 2559-2564.
- LAZAREV, A.N. (1972): *Vibrational Spectra and Structure of Silicates*. Consultant Bureau, New York, N.Y.
- LEWIS, I.R., CHAFFIN, N.C., GUNTER, M.E. & GRIFFITHS, P.R. (1996): Vibrational spectroscopic studies of asbestos and comparison of suitability for remote analysis. *Spectrochim. Acta A* **52**, 315-328.
- LOH, E. (1973): Optical vibrations in sheet silicates. *Solid State Phys.* **6**, 1091-1104.

- MELLINI, M. (1982): The crystal structure of lizardite-1T: hydrogen bonds and polytypism. *Am. Mineral.* **67**, 587-598.
- _____ & VITI, C. (1994): Crystal structure of lizardite-1T from Elba, Italy. *Am. Mineral.* **79**, 1194-1198.
- PASTERIS, J.D. & WOPENKA B. (1987): Use of a laser microprobe to trace geological reactions. *Microbeam Analysis*, 205-209.
- ROSASCO, G.J. & BLAHA, J.J. (1980): Raman microprobe spectra and vibrational mode assignments of talc. *Appl. Spectrosc.* **34**, 140-144.
- VEBLEN, D.R. & WYLIE, A.G. (1993): Mineralogy of amphiboles and 1:1 layer silicates. *In Health Effects of Mineral Dusts* (G.D. Guthrie Jr. & B.T. Mossman, eds.). *Rev. Mineral.* **28**, 61-137.
- WICKS, F.J. & O'HANLEY, D.S. (1988): Serpentine minerals: structures and petrology. *In Hydrous Phyllosilicates (Exclusive of Micas)* (S.W. Bailey, ed.). *Rev. Mineral.* **19**, 91-167.
- _____ & WHITTAKER, E.J.W. (1975): A reappraisal of the structures of the serpentine minerals. *Can. Mineral.* **13**, 227-243.

Received December 8, 2002, revised manuscript accepted June 23, 2003.